



Open Archive TOULOUSE Archive Ouverte (OATAO)

OATAO is an open access repository that collects the work of Toulouse researchers and makes it freely available over the web where possible.

This is an author-deposited version published in : <http://oatao.univ-toulouse.fr/>
Eprints ID : 9249

To link to this conference :

URL : <http://dx.doi.org/10.3182/20120902-4-FR-2032.00066>

To cite this version : Roboam, Xavier and Sareni, Bruno and Nguyen, Duc Trung and Belhadj, Jamel. *Optimal system management of a water pumping and desalination process supplied with intermittent renewable sources*. (2012). In: 8th Power Plant and Power System Control Conference, 02-05 Sep 2012, Toulouse, France.

Any correspondence concerning this service should be sent to the repository administrator: staff-oatao@listes-diff.inp-toulouse.fr

Optimal System Management of a Water Pumping and Desalination Process Supplied with Intermittent Renewable Sources

ROBOAM Xavier*, SARENI Bruno*, NGUYEN Duc Trung*, BELHADJ Jamel**

* Université de Toulouse, LAPLACE (Laboratory on Plasma and Conversion of Energy), UMR CNRS-INPT-UPS, site ENSEEIHT, 2 rue Charles Camichel BP 7122, 31071 Toulouse, France
e-mail: {dtnguyen, sareni, roboam}@laplace.univ-tlse.fr).

** Université de Tunis ElManar, Laboratoire des systèmes électriques (LSE) ENIT BP 37, Le Belvédère 1002 Tunis, Tunisie. Jamel.Belhadj@esstt.rnu.tn

Abstract: this paper aims at defining energy management strategy for a water pumping and desalination process which would be powered by a hybrid (solar PV & wind) renewable generation system. Several pumping subsystems for well pumping, water storage and desalination are coupled. The particularity of the proposed architecture with its management deals with the absence of electrochemical storage, only taking benefit of hydraulic storage in water tanks: in such an autonomous device, given a certain level of intermittent power following wind and sun irradiation conditions, and given hydraulic characteristics of water pumping subsystems, this study puts forward the prime importance of a water and power flow management optimization. For this purpose, both dynamic and quasi static models are proposed before setting the management strategy based on optimal power dispatching. Subsequent results are analyzed in terms of robustness and performance.

Keywords: energy management, autonomous system, renewable energy, intermittent power, desalination, Bond Graph, optimization.

1. INTRODUCTION

Many dry regions and isolated areas of the world have to face the issue of water, especially fresh water scarcity (Turki et al., 2008). The use of autonomous water pumping and desalination units supplied by renewable energy sources can be a viable solution for remote areas, where there is sometimes no access to the electrical grid, but where renewable energy resources based on sun and/or wind power are abundant (Kalogirou et al., 2005; Koklas et al., 2006). Such autonomous systems (see Fig.1) are characterized by an *intermittent* generated power 'given' or offered along wind speed and solar irradiation conditions. On the other way, the *load characteristics* are also *set* for all subsystems here constituted of motor pumps, desalination process and hydraulic network (pipes and vales). More generally, this class of autonomous systems with intermittent input power for generation and given characteristics for loads are more and more spread in modern systems as in smart grids or renewable energy processes. Such class of standalone system requires a specific and optimized management for power and material flows: here water, but hydrogen or thermal flows for other cases of process (Ben Rhouma et al., 2008). The issue is always to take benefit of the given power from an impedance adaptation given load characteristics. Usually, storage devices (i.e. flywheels, ultracapacitors, accumulators or H₂/O₂ storage) are used and specifically sized to decouple the intermittent power generation and the power needs for loads. But the owning cost of such storage devices due to investment costs and life duration are sometimes excessive so

that minimizing or even suppressing storage devices should be a challenge. For our case study, the issue is then to minimize electrical storage only using a capacitor (at maximum a ultracapacitor) to stabilize the DC bus link. Our idea is to take benefit on the one hand of hydraulic storage in water tanks and, on the other hand to exploit modularity (several pumping subsystems that can be switched on/off and tuned). In such a case, the intermittent power 'given' by generators has to be dispatched in all subsystems: an optimization strategy is then necessary for maximizing their efficiency characteristics and fulfilling technological (power and pressure ranges) and functional constraints (tank filling).

This paper then proposes a first approach for water production optimization based on specific modeling and management strategy. First, after having set the problem, a dynamic model based on Bond Graph formalism is compared with a quasi static model for validation. Being very rapid to simulate, this latter model is well suited for long term representation of complex systems, especially as the optimization process requires a large number of system runs to converge. Then, we will see that setting the objective function is not so obvious for this class of problem: five different objective functions are then compared in terms of robustness and performance. The influence of system environment (here the power cycles related to wind and sun conditions) is also analyzed, being strongly coupled with system efficiency. Finally, the effect of device sizing, especially for motor pumps, is also analyzed, which put forward the necessity of a 'systemic optimal design' integrating simultaneously couplings between architecture (modularity), sizing and flow (power, water) management.

2. PROCESS MODELING

As previously introduced, the considered system is constituted of renewable energy generation system (presented in details in Dali et al., 2009) coupled through a DC link with several water pumping and desalination subsystems as illustrated in the synoptic of Fig.1. Those processes and the corresponding dynamic models have been characterized in previous studies (Ben Rhouma et al., 2008; Turki et al., 2008) through two experimental test benches of LSE Lab facilities (see Fig 2).

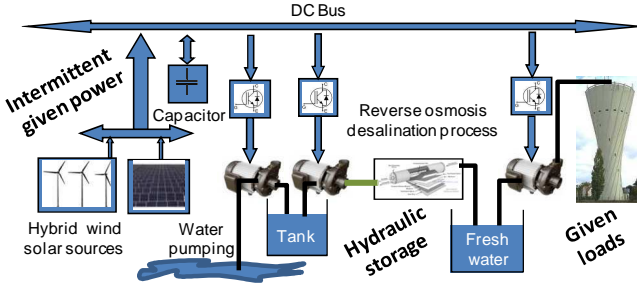


Fig. 1. Synoptic of the autonomous water process system

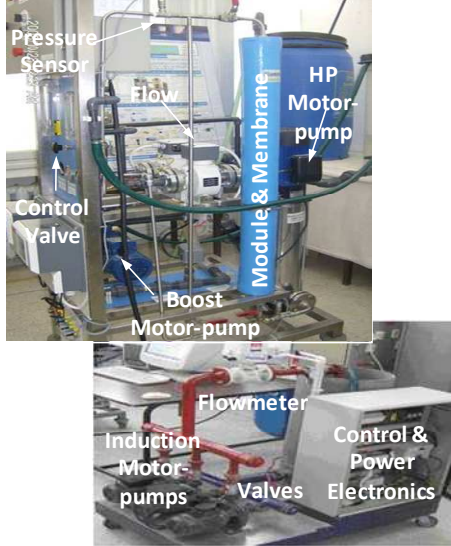


Fig. 2. Water desalination and pumping experiments

In these studies, we have considered the Bond Graph (BG) formalism (Karnopp et al., 2000), especially adapted for dynamic modeling of multidisciplinary energy systems. Energy based analogies between physical models are considered: for example a **C** element characterizes a potential storage, as for an electrical Capacitor, a mechanical Compliance or a hydraulic tank. Power variables (effort-flow) are supported on bonds, respectively corresponding to voltage-current in electricity, force (or torque) and speed in mechanics and pressure-flow in hydraulic devices.

2.1. The RO (Reverse Osmosis) desalination module

The desalination device involves several power losses in pipes (with its restriction R_{pipe}), RO membrane, and in the controllable rejection valve (with variable restriction R_{valve}) at the output of the rejected salted water. This process is an example of multidisciplinary device coupling chemical, thermal and hydraulic flows (Turki et al., 2008). However, in order to achieve the energy management of the whole system,

a reduced 'full hydraulic' model can be extracted in which the membrane is composed of a **C** element (usually also neglected) and a **R** variable phenomenon (R_{memb}) depending on the membrane conductivity. The feed flow is then shared between the fresh water flow (i.e; the permeate $Q_{permeate}$) and the rejected water (i.e; the concentrate $Q_{concentrate}$). In our case, we consider brackish water with very small concentration so its osmotic pressure is neglected. A dynamic equivalent hydraulic circuit and its corresponding Bond Graph are displayed in Fig. 3.

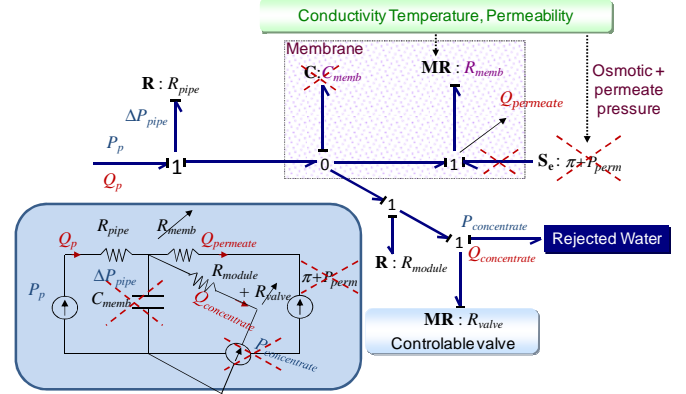


Fig. 3. Equivalent hydraulic circuit and BG of RO module.

From this dynamic BG, a quasi static model of the RO module can be expressed, neglecting the storage effect in C_{memb} (due to the high 'stiffness' of the membrane) and the output pressures of permeate and concentrate circuit:

$$P_p - \Delta P_{pipe} = (R_{module} + R_{valve}) Q_{concentrate}^2 \quad (1)$$

$$Q_{permeate} = \frac{P_p - \Delta P_{pipe}}{R_{membrane}} \quad (2)$$

$$Q_p = Q_{permeate} + Q_{concentrate} \quad (3)$$

where P_p , $Q_{concentrate}$, $Q_{permeate}$, Q_p are respectively the output pressure of the high pressure pump, the flow of the rejected water (concentrate), the flow of the fresh water (permeate), and the input flow feed from the pump.

2.2. The pump model

In the same way, a dynamic BG model can be established for the centrifugal pump (see Fig. 4). In this model P_p , T_m , Ω , Q_p are respectively the output pressure and flow of the pump, the motor torque and speed. The mechanical-hydraulic power conversion is modeled by a nonlinear gyrator (see Eq. 4,5) with a and b coefficients (Turki et al., 2008).

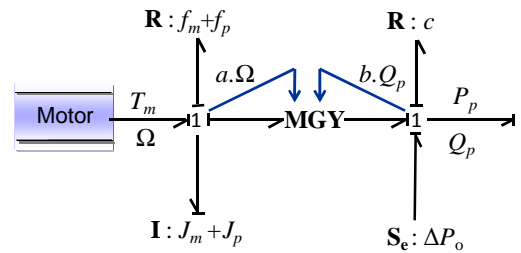


Fig. 4. BG of the centrifugal pump

During the pump operation, some losses and dynamic effects appear because of the suction pressure (ΔP_0), hydraulic friction (c), and motor-pump mechanical inertia and losses

$(J_p + J_m, f_p + f_m)$ (Gülich, 2008). By neglecting the $J_p + J_m$ equivalent inertia effect, the *static part* of the motor-pump model can be expressed as:

$$P_p = (a\Omega + bQ_p)\Omega - (cQ_p^2 + \Delta P_0) \quad (4)$$

$$T_m = (a\Omega + bQ_p)Q_p + (f_m + f_p)\Omega \quad (5)$$

The pump parameters ($a, b, c, f_m + f_p, \Delta P_0$) can be extracted from experiments or from manufacturer data sheets.

2.3. The pipe model

The pressure drop in the pipe is composed of dynamic and static pressure (Gülich, 2008):

$$\Delta P_{pipe} = P_{dynamic} + P_{static} = KQ_p^2 + \rho gh \quad (6)$$

h being the height of water pumping and ρ the water density.

2.4. The DC equivalent motor model

Classically, centrifugal pumps are driven by Field Oriented Controlled (FOC) inverter fed induction motors (Sul, 2011). If only the energetic behavior is concerned in order to optimize the system management strategy, a simplification should be to consider an equivalent chopper fed DC machine of which parameters are calculated to set the equivalence with the induction motor drive. Then, a BG of this converter motor device can be obtained while simple motor equations are established for the quasi static model by neglecting the motor inertia:

$$V_m = R_m I_m + \Phi_m \Omega \quad (7)$$

$$T_m = \Phi_m I_m \quad (8)$$

where T_m and Ω are respectively the motor electromagnetic torque and the rotation speed, Φ_m is the torque equivalent coefficient, R_m is the stator resistance. Then, the electrical power P_e can be expressed from (7) and (8) as:

$$P_e = V_m I_m = \left(R_m \frac{T_m}{\Phi_m} + \Phi_m \Omega \right) \frac{T_m}{\Phi_m} \quad (9)$$

2.5. Whole system modeling

Finally, for the case of the RO subsystem with the HP pump, the whole dynamic BG model is displayed in Fig. 5 in which several series connected elements have been merged as for pump and pipe's **R** elements and effort sources. Note that the model is nearly the same for pumping subsystems, except of the hydraulic load which slightly differs.

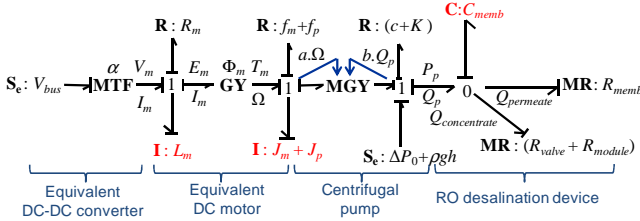


Fig. 5. BG of the whole system

The global static model can be established by neglecting **I** and **C** dynamic elements (in red color). In case of pumping operation with no hydraulic load, the motor-pump speed Ω can be derived from (4) and (6) by choosing the positive root of the 2nd order equation:

$$\Omega(Q_p) = \frac{-bQ_p + \sqrt{(bQ_p)^2 + 4a[(c + K)Q_p^2 + \Delta P_0 + \rho gh]}}{2a} \quad (10)$$

The motor torque T_m can then be expressed versus the pump flow Q_p from (5) and the electrical power P_e (system input) can be found from (9).

Similarly, in case RO desalination, the pump pressure P_p can be expressed versus the pump flow Q_p considering the hydraulic load defined by (1), (2), (3), and (6). A nonlinear expression of the electrical power P_e versus Q_p is found by combining (4), (5) and (9).

3. CHARACTERIZATION OF DYNAMIC AND STATIC MODELS

The static model strongly reduces the simulation time for such system. This model reduction is all the more important than an optimization approach is necessary for the power dispatching strategy. In this case, several system simulations have to be performed to reach an optimum value. The dynamic model of Fig. 5 is implemented in the 20-Sim[®] BG solver. The quasi static model is coded in Matlab[®] software. Equation (9) can be inverted by using the “fsolve” function for calculating the pump flow versus the input electrical power. In order to compare the dynamic and quasi-static models, the simplified structure of Fig. 6 is proposed with a well pump and a high pressure pump for desalination.

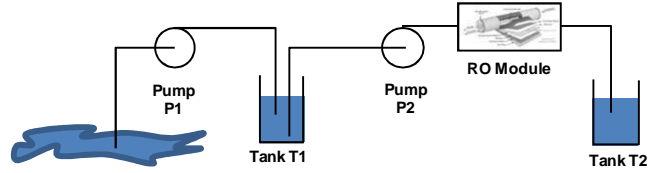


Fig. 6. System configuration for BG/static model comparison

All tests are based on two pumps from Grundfos:

- The pump P1 (well pump) is rated at 1.5 kW (type SP 5A-17): to feed water to the T1 tank,
- The pump P2 (HP pump for RO) is rated at 2.2 kW (type SP 5A-25) to increase the pressure from T1 to T2 through the RO module. The RO module includes one element (TM710) from TORAY with one pressure body (PV-3110).

Table 1. Grundfos pump parameters

Pump Parameters	P1 (SP 5A-17)	P2 (SP 5A-25)
a (Ns ² /m ²)	10.87	13.74
b (Ns ² /m ⁵)	-6251	-20010
c (Ns ² /m ⁸)	1.839×10^{11}	2.193×10^{11}
$f_m + f_p$ (Nms)	0.0043	0.0050
ΔP_0 (N/m ²)	2124	14200

Table 2. The RO module parameters

R_{memb} (Ns/m ⁵)	$1.695 \cdot 10^{10}$
R_{module} (Ns ² /m ⁸)	$1.038 \cdot 10^{12}$
R_{valve} (Ns ² /m ⁸)	$7.785 \cdot 10^{12}$

The initial level of both tanks (T1 and T2) is 0.2 m. The input power (see Fig.7) is distributed into two equal parts to both pumps (i.e 50% of power sharing factor).

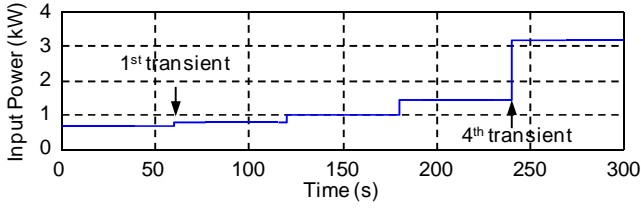


Fig. 7. Input power used for model comparison

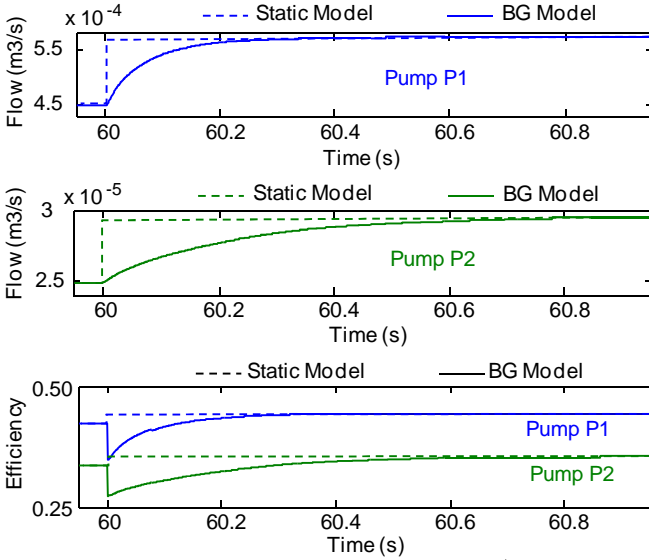


Fig. 8. Difference between models during the 1st transient

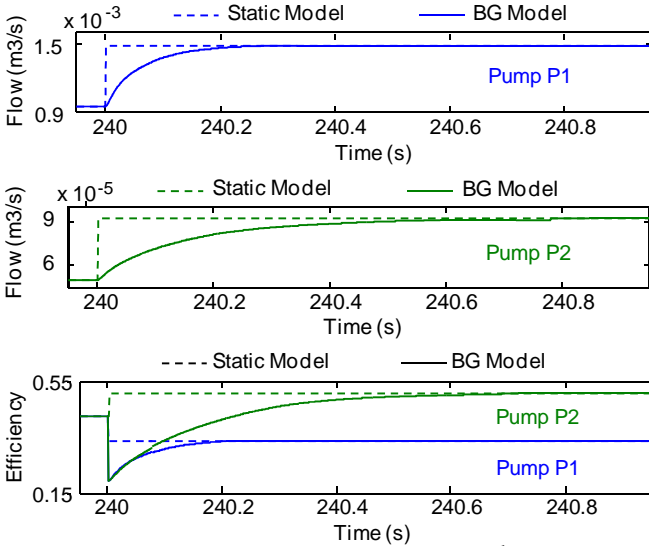


Fig. 9. Difference between models during the 4th transient

The resulting difference between both dynamic and quasi static models is not significant in terms of power/energy balance over a wide range of operation. A small difference only occurs at transients as illustrated in Fig. 8 and Fig. 9 (note that results are also the same for second and third transients). Finally, the reduced quasi static model is considered as acceptable in order to optimize the system management which allows reducing significantly the convergence time of optimization as presented in the next section.

4. WATER MANAGEMENT STRATEGY

4.1. Setting the problem of water management

This section sets the problem to be solved in order to simultaneously manage power and water flows with a maximum efficiency during the system operation. We still use the simplified configuration as in Fig. 6 with the input power of Fig. 10. We show in Fig. 11 and in Table 3 the water level stored in both tanks when this power is dispatched according to different power sharing factor α_p defined as:

$$\alpha_p = \frac{P_{e1}}{P_{in}} = \frac{P_{e1}}{P_{e1} + P_{e2}} \quad (11)$$

where P_{e1} and P_{e2} denotes the electrical powers feeding respectively the pump P1 and the pump P2, P_{in} is the input power to be dispatched. It can be seen from Table 3 and Fig. 11 that different water levels can be obtained in each tank according to the α_p value. In the first case ($\alpha_p = 0.2$), the increase of total level is the smallest because the pump P1 operates in the region of low efficiency with very low input power. This example emphasizes the *first coupling* between power and subsystems efficiency: the generated power from renewable sources is then strongly coupled with the water process system efficiency. In particular, the importance of respecting pumping power limits to prevent problematic operations that degrade efficiency and that could also reduce the life duration of pumps. The last case ($\alpha_p = 0.5$) gives the best result because both pumps operate with good efficiency.

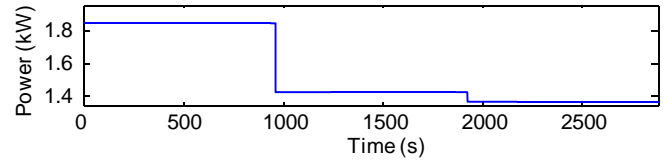


Fig. 10. Input power used for showing the influence of the energy management based on power dispatching

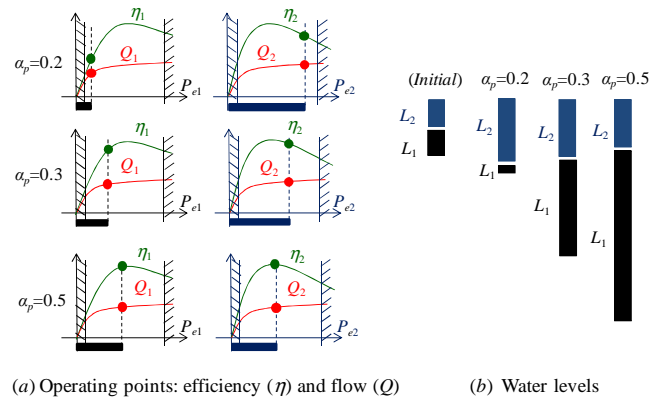


Fig. 11. Water levels obtained from various operating points corresponding to different power sharing factors

Table 3. Tank levels for different power sharing factors

Level (m)	Initial value	$\alpha_p=0.2$	$\alpha_p=0.3$	$\alpha_p=0.5$
Level of T1	0.2	0.114	0.893	1.992
Level of T2	0.2	0.418	0.397	0.351
Total level	0.4	0.532	1.29	2.343
Level gap	—	0.132	0.89	1.944

Note that this result is only related to a particular sizing of the two pumps (here respectively 1.5 and 2.5 kW). Modifying its sizing should also vary the system performance: this latter issue emphasizes the *second coupling* between sizing and management performance. A *third coupling*, between tank level and power management has also to be managed: indeed, after a certain operation time, the maximum level of tanks can be attained. On the opposite, operating the pumps P2 is only possible if the tank T1 is not empty. Based on this strongly coupled system design (water management and pump sizing), the next subsection aims at optimizing the operation and especially the power dispatching strategy.

4.2. Formulation of the optimal power dispatching

In the following, we will consider a more complete system with 3 pumps, corresponding with the synoptic of Fig.1 and displayed in Fig. 12. All tanks have the same volume with a base area of 1 m^2 and a height of 2 m. The initial level of all tanks is set at: 1m for T1, 0.2 m for T2 and 0.2 m for T3.

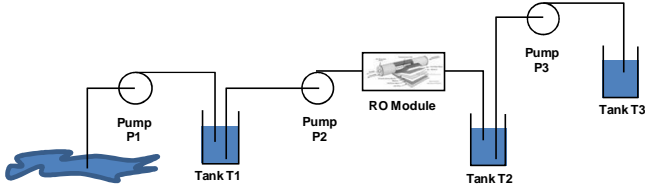


Fig. 12. Desalination system base on RO module

The input power is sampled every 10 min. At each sample, a dispatching algorithm is performed in order to share the input power between all pumps, while ensuring operating constraints: in particular, the shared power assigned to each pump has to be bounded by pump technological limits (i.e. $P_{e\min} \leq P_e \leq P_{e\max}$) and the level L in each tank has to lie in the interval $L_{\min} \leq L \leq L_{\max}$ corresponding to the capacity limits. Each of the three pumps having two possible operating states S_p (i.e. $S_p = 1$ or $S_p = 0$ respectively for on/off operations), eight possible states $S = S_{p3}S_{p2}S_{p1}$ are *a priori* feasible at every sampling period (from $S = 000$ to $S = 111$). The dispatching algorithm first identifies the number of possible states, i.e. which pump can be switched according to the input power range conditions and to the current levels of the tanks. For example, if the tank T3 is full, the pump P3 has to be switched off and only four states are feasible (from $S = 000$ to $S = 011$). Then, for each feasible state a second step is performed consisting in optimizing the input power dispatching. The optimal dispatch problem can be formulated into the following constrained optimization problem:

$$\begin{cases} \max_{\mathbf{x} = Q_{p1}, Q_{p2}, Q_{p3}} f_{obj}(\mathbf{x}) \\ P_{ei\min} \leq P_{ei} \leq P_{ei\max} & i = 1..3 \\ L_{i\min} \leq L_i \leq L_{i\max} & i = 1..3 \end{cases} \quad (12)$$

where the objective function to be maximized should represent the efficiency of the energy and flow transfers in the system. Such problem can be solved using standard nonlinear programming methods (typically by means of *fmincon* Matlab function). Note also that pump flows Q_{pi} are used for the decision variables instead of the corresponding shared electrical power P_{ei} in order to avoid the inversion

of (9). Each feasible state leads to an optimal objective function and the best value obtained among all states is returned. The corresponding power values for switched on pumps are considered as power references. In this particular problem, the choice of the objective function is not obvious. Indeed the issue is to minimize the time needed to fill the superior tank T3. Then, given a certain input power fed by the renewable intermittent sources, the power dispatching strategy has to pay attention of energy efficiency of the three pumps but also of the tank levels: five different objective functions are proposed and compared in the next subsection.

4.3. Proposed objective functions for the dispatching strategy

The f_1 objective function deals with the system efficiency:

$$f_1 = \frac{P_{out}}{P_{in}} = \frac{\sum_{i=1}^3 P_{hydraulics}}{P_{in}} = \frac{\sum_{i=1}^3 P_{pi} Q_{pi}}{P_{in}} \quad (13)$$

The f_2 objective function aims at maximizing the total flow:

$$f_2 = \sum_{i=1}^3 Q_{pi} \quad (14)$$

The f_3 objective function is the same as f_3 but with weighting coefficients depending on the tank level:

$$f_3 = \sum_{i=1}^3 \omega_i Q_{pi} \quad \text{where} \quad \omega_i = \frac{L_{i\max} - L_i}{L_{i\max} - L_{i\min}} \quad (15)$$

The f_4 objective function is similar to f_3 but with quadratic flows:

$$f_4 = \sum_{i=1}^3 \omega_i Q_{pi}^2 \quad (16)$$

Finally the f_5 objective function aims at maximizing the output hydraulic powers as for f_1 but with weighting coefficients ω_i linked with tank levels similarly to (15):

$$f_5 = \sum_{i=1}^3 \omega_i P_{hydraulics} = \sum_{i=1}^3 \omega_i P_{pi} Q_{pi} \quad (17)$$

The proposed objective functions need to be tested with different input power waveforms. The criterion to compare the objective function robustness is the “finishing time”, that means the time needed to fill the three tanks T1, T2 and T3 (with 2 m of height for everyone) from an initial level of 1 m for T1, 0.2 m for T2 and 0.2 m for T3.

4.4. Results and analysis

All tests have been applied with three waveforms of input power.

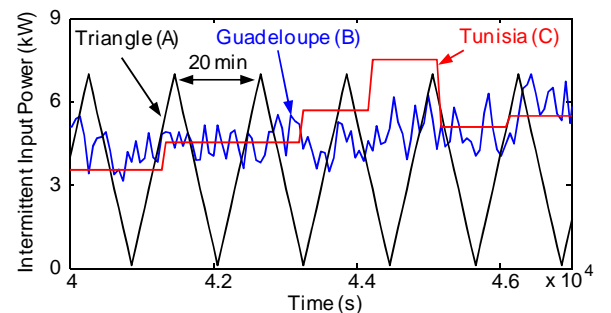


Fig. 13. Zoom on three waveforms of input power

The first waveform (A) is for an input power with a theoretical triangle shape. The second waveform (B) corresponds to an intermittent power issued from wind turbine measurements in Guadeloupe (with small sampling period). Similarly, the third waveform (C) is relative to a power cycle extracted from wind turbines in Tunisia (with higher sampling period). In the following, the amplitude of the input power waveform is multiplied by several reduction factors k varying from 0.45 to 0.7 in order to analyze the coupling between the system environment (i.e. the shape and the amplitude of the given input power) and the system efficiency. It can be observed from Table 4 that the most appropriate objective function is f_5 (column in bold type in Table 4) which corresponds to the maximization of the output power weighted with the level of the tanks. This objective function can also be considered as robust versus input profiles as it always offers the smallest finishing time whatever the power waveform and its reduction factor k .

Table 4. Finishing time (in min) for different objective functions

Input Power	f_1	f_2	f_3	f_4	f_5
A ($k = 0.7$)	637	652	635	628	618
B ($k = 0.7$)	590	597	597	602	574
C ($k = 0.7$)	814	823	815	815	804
A ($k = 0.55$)	777	765	733	732	718
B ($k = 0.55$)	698	700	694	716	689
C ($k = 0.55$)	883	902	892	897	878
A ($k = 0.5$)	787	809	778	794	776
B ($k = 0.5$)	745	740	739	763	732
C ($k = 0.5$)	932	939	929	948	917
A ($k = 0.45$)	852	887	852	875	851
B ($k = 0.45$)	797	786	788	812	784
C ($k = 0.45$)	996	1013	1001	1008	980

5. INFLUENCE OF THE PUMP SIZING ON THE SYSTEM EFFICIENCY

This section aims at analyzing the coupling effect between sizing and system management. Only the most robust objective function f_5 is used in that part in order to test different combinations of motor pump sizing. These combinations include electrical converters, electrical motors and pumps. Several combinations with rated powers from 1.5 kW to 11 kW are displayed in Table 5. Only the waveform C of the input power from Tunisia with three different reduction factors k is considered.

Table 5. Finishing time (in min) for different sizing

Rated powers of P1, P2, P3*	C $k = 0.7$	C $k = 0.55$	C $k = 0.5$
(1.5 kW 1.5 kW 1.5 kW)	914	965	985
(1.5 kW 2.2 kW 1.5 kW)	804	878	917
(1.5 kW 4.0 kW 1.5 kW)	801	898	879
(1.5 kW 7.5 kW 1.5 kW)	757	827	886
(1.5 kW 11 kW 1.5 kW)	748	840	938

*Reference of used pumps from Grundfos manufacturer: 1.5kW – SP5A-17; 2.2kW – SP5A-21; 4kW – SP5A 44N; 7.5kW – SP 5A 75; 11kW – SP8A 73.

Best results (i.e. the smallest finishing time) are indicated in bold type in this table. As we can observe, it is necessary to investigate the sizing of the three pumps combination to get an optimal system design. It is interesting to note that the smaller the amplitude of input power (i.e. when k decreases), the smaller the optimal rated power for the combination of pumps. It should also be noted that there is a strong coupling between sizing and environment profile (i.e. shape and intensity of the input power).

6. CONCLUSIONS

In this paper, the energy management of a water pumping and desalination process has been studied. Based on a quasi static model validated with a dynamic BG model, an optimal dispatching strategy has been proposed for sharing the intermittent input power between different pumps. In particular, the choice of the objective function used in this strategy for assessing the operating efficiency has been analyzed. It is shown that a robust solution consists in taking as objective function the sum of hydraulic powers weighted by the associated tank levels. On the other hand, the influence of the pump sizing on the system efficiency is also underlined. This justifies new studies in order to investigate global optimization approaches taking account of the couplings between the system architecture, sizing and energy management.

REFERENCES

- Ben Rhouma A., Belhadj J., Roboam X. (2008). Control and energy management of a pumping system fed by hybrid Photovoltaic-Wind sources with hydraulic storage. *Journal of Electrical Systems*, Vol. 4, 1–16.
- Charcosset C. (2009). A review of membrane processes and renewable energies for desalination. *Desalination*, Vol. 245, 214–231.
- Dali M., Belhadj J., Roboam X. (2009). Hybrid wind-photovoltaic power systems: Structure Complexity and Energy Efficiency, Control and Energy management. *EJEE RIGE*, Vol. 12, 669–700.
- Gülich. J.F. (2008). *Centrifugal Pumps*, 964. Springer, Verlag Berlin Heidelberg, New York.
- Kalogirou. S. A. (2005). Seawater desalination using renewable energy sources. *Progress in Energy and Combustion Science*, Vol. 31, 242–281.
- Karnopp D., Margolis D., Rosenberg R. (2006), *System Dynamics: Modeling and Simulation of Mechatronic Systems*, 563. John Wiley & Sons, Hoboken.
- Koklas P.A., Papathanassiou S.A. (2006). Component sizing for an autonomous wind-driven desalination plant. *Renewable Energy*, Vol. 31, 2122–2139.
- Sul S. K. (2011). *Control of Electric Machine Drive System*, 399. John Wiley & Sons, Hoboken, New Jersey.
- Tanaka, K., Rong, W., Suzuki, K., Shimizu, F., Hatakenaka, K., and Tanaka, H., (2000) Detailed Bond Graph of Turbomachinery. *IEEE IECON*, 1550–1555.
- Turki M., Belhadj J., Roboam X., (2008). Control strategy of an autonomous desalination unit fed by PV-wind hybrid system without battery storage. *Journal of Electrical Systems*, Vol. 4, 1–12.